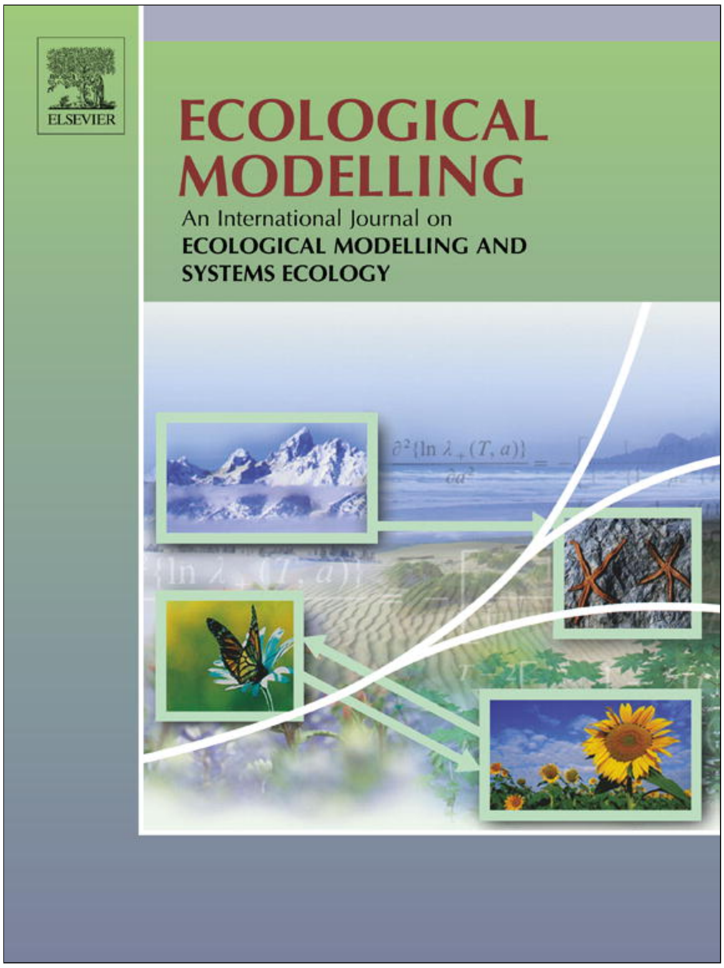

ELSEVIER
ECOLOGICAL MODELLING
An International Journal on
ECOLOGICAL MODELLING AND SYSTEMS ECOLOGY

Ecological Modelling 237–238 (2012) 74–87

Contents lists available at SciVerse ScienceDirect

Ecological Modelling

journal homepage: www.elsevier.com/locate/ecolmodel

A “Matchstick Model” of microwave backscatter from a forest

Matthew Brolly[a],*, Iain H. Woodhouse[b]

[a] Department of Geographical Sciences, University of Maryland, College Park, MD, USA
[b] School of GeoSciences, The University of Edinburgh, United Kingdom

ARTICLE INFO

Article history:
Received 12 September 2011
Received in revised form 13 April 2012
Accepted 14 April 2012

Keywords:
Vegetation
Forestry
Synthetic aperture radar
Biomass
Backscatter

ABSTRACT

Given that the majority of biomass is contained in the stems of trees within forests (as much as 90%), a new radar modelling approach is proposed here wherein the stems are the major biomass contributor in the context of Synthetic Aperture Radar backscatter sensitivity to forest biomass. The new model regards stems are as “matchsticks” consisting of constant radius, constant density, and constant dielectric properties. Furthermore, by considering only the larger constituents of the forest a clearer understanding of the correlation of biomass with backscatter from P and VHF Band SAR can be obtained.

Using backscatter data, and specifically the trends, produced from the RT2 radiative transfer model this paper considers the effects of SAR scattering when interacting with forest stands consisting of identical vertical stems, or matchsticks. SAR frequencies of 50 MHz (VHF) and 429 MHz (P Band) are used to generate a comparative radar interaction data. These not only allow a comparison of the scattering of SAR signals of different wavelengths but also of how interactions with stems can reveal novel clues as to the source of the backscatter saturation phenomenon of forests. Removing the random volume scattering aspect of a forest, the canopy, would be expected to eliminate the saturation behaviour which occurs at increasing levels of biomass density, an effect believed to be due to extinction effects, but is shown here to not be the case. Results reveal that saturation behaviour can occur even for the low number density case where increasing the size of stems through the radii associated with Rayleigh, Mie and Optical scattering will result in backscatter saturation as the biomass density is increased. Consistent with this finding, a forest of solely vertical stems will exhibit saturation behaviour at lower biomass density values when lower planting densities of similar stems are used. In this study the backscatter model considers the ground contribution to be negligible but does include the double bounce as a result of interactions between the stems and ground.

Also considered are Mie backscatter oscillations which are shown to average out when using both non-vertical stems and random radius values about a mean, both independently and collectively. These “Mie” effects can also be removed by altering the incident SAR angle. These findings allow a reduction of the backscattering scenario of forests to a two-region problem involving solely Rayleigh and Optical scattering. This serves to further provide an explanation as to the origin of saturation, whereby the balance between the Optical scattering increase and the matchstick number density decrease cancel each other out.

The important conclusion is that backscatter does not measure biomass, but measures structural trends that are correlated with biomass in different ways, driven by stand level competition, resource use, etc. As a result different forest growth regimes should expect different backscatter–biomass trends.

1. Introduction

Modelling vegetation as a random volume over a ground (RVoG) provides a simple, deductive tool for understanding microwave backscatter from a forest (Treuhaft et al., 1996). It forms the basis of height determination from polarimetric interferometry (Papathanassiou and Cloude, 2001) and, with its history in the Water Cloud Model (Attema and Ulaby, 1978), continues to support the widely held assumption that saturation of backscatter with increasing biomass is always driven by increased canopy opacity. However, these models fail to capture one key physical aspect of a forest, namely that the stems, especially in conifer species, often contain the majority of the standing biomass (up to 90% according to a study of 332 angiosperm and 343 conifer dominated communities (Cannell, 1982)), and similarly for tropical species (Bastien-Henri et al., 2010). This is important for two reasons: (1)

---

* Corresponding author at: Department of Geographical Sciences, LeFrak Hall, University of Maryland, College Park, MD 20742, USA. Tel.: +1 202 3404052.
E-mail addresses: MBrolly@umd.edu (M. Brolly), I.H.Woodhouse@ed.ac.uk (I.H. Woodhouse).

0304-3800/$ – see front matter © 2012 Elsevier B.V. All rights reserved.
http://dx.doi.org/10.1016/j.ecolmodel.2012.04.014

at long wavelengths (P-band and longer) stems make a significant contribution to the total backscatter (Smith and Ulander, 2000; Smith-Jonforsen et al., 2007), and (2) that total backscatter within an area is determined by the number of stems as well as their individual shapes and sizes (Smith-Jonforsen et al., 2007; Imhoff, 1995b). While backscatter increases with increasing stem size, an increase in biomass can typically be associated with a corresponding rapid decrease in the number density of stems (Niklas et al., 2003).

In order to understand the balance of these conflicting trends, this paper introduces a new deductive model of forest backscatter based on a collection of identical cylindrical stems, with no canopy. By combining the simplified representations of the backscatter trends from individual stems based on earlier models (Smith and Ulander, 2000; Fransson et al., 2000b, 2004), with the generalised stem dynamics observed in macroecological studies (West et al., 1999), this model is able to explain the range of observed backscatter–biomass trends published in the last 30 years. This "Matchstick" model approach to simplify the forest structure builds on more generalised applications of macroecological studies in backscatter modelling by Woodhouse (2006). Our key question is as follows: is radar backscatter a good indicator of stem volume (biomass) per unit area when only the tree stems are considered? The concept that "structure" may influence backscatter is not new (see Imhoff, 1995b, for example) but here we expand this concept to introduce a formalised model at the stand level based on generalised biological principles.

The validity of the model and its limitations are demonstrated by comparing model predictions to both radiative transfer model results and previous empirical studies at VHF, and P Band (50 MHz, 429 MHz). Understanding the trends in radar backscatter measurements of forests is undeniably important from scientific, economic and policy related standpoints, since one of the most important applications of remote sensing is the monitoring of forests and their contribution to the terrestrial carbon cycle and related policy issues, such as REDD (Gibbs et al., 2007).

2. Methods and theory: the Matchstick Model

Simple, single layer models of microwave scattering from a forest have treated the target surface as either a dielectric slab with constant properties suspended above the ground (Bush and Ulaby, 1976) or a layer of sparsely distributed identical dielectric scatterers. These scatterers can be spheres, as in the Water Cloud Model (Attema and Ulaby, 1978), or random cylinders (Peake, 1959) which may be randomly oriented, (now referred to as the Random Volume Over Ground (RVOG) model (Papathanassiou and Cloude, 2001; Mette et al., 2004)) or with a systematic orientation (Treuhaft et al., 1996; Smith et al., 2002). These models share one important common feature in that none of them considers the change in number density of tree stems associated with biomass changes – this is the same effect as the "consolidation" described by Imhoff (1995b) and significantly influences the backscatter and its trends even if the volume remains the same. The referred models *do* include the extinction as a free parameter, which could include the impact of tree density but this is not the same as explicitly including number density.

Therefore, remaining within the tradition of simple, single-layered models, we describe here a model based on a single layer of stems, which we call the "Matchstick Model". It is an oriented layer of cylinders and as such the model is most suited to P-band wavelengths or longer. The stems are identical and always (near) vertical, and do not account for tapering. The forest biomass is assumed to be directly proportional to the total volume of the cylinders in a similar fashion to the relationships explored in Fang et al. (1998) in which a simple linear relationship between stand biomass and volume is shown to exist for all the main forest types in China, albeit slightly underestimating biomass. Similar relationships are found in Valentine et al. (1984), Philip (1994) and Le Toan et al. (2002). Changes in area biomass are therefore a result of changes in total cylinder volume. Since the stem volume–biomass relationship is expected to be both species and site specific, our primary application of the model is to explore *trends* in backscatter associated with biomass changes (rather than simulate absolute values). A visual representation of the model is demonstrated in Fig. 1. In part, the purpose of this model is to take a very different stance from the models referenced above which are widely used both for explanation and inversion tools, yet often take no account of the variability and progressive change in the size distribution. This single layer model, with each layer comprising equally sized cylinders changing with age, uses stem-sized cylinders as the representative scatterer while maintaining the single layer simplicity of previous models.

Sections 2.1 and 2.2 describe how the changes in stem size and number density can be characterised using general macroecology principles. The two following sections describe the comparative modelling approach: first, the simple model that encapsulates trends in backscatter from varying sized stems, followed by a corroboration of these trends using a full radiative transfer model. In each case the modelled scenario is that of a developing forest with increasing biomass. We assume that differences in time can also be used as a surrogate for spatial variability. This is most relevant in a plantation scenario. However, modelling a single stand across a number of years does not take account of variations in terms of ground conditions and other environmental factors that may directly affect the growth of the forest. In spite of this, this method allows a direct analysis of the effect of size and number distribution on the trends of radar backscatter. This method of forest modelling is therefore most relevant to studies where a wide range of biomass values are acquired over varying stages of growth. This is particularly true within monospecies stands in which the allometry of individual trees is assumed to vary very little, and resource levels to remain fairly consistent across neighbouring stands.

2.1. Individual stem characteristics

In this study the variables that determine individual stem sizes are (1) a scaling factor, a, which determines proportional change of cylinder shape to cylinder size (West et al., 1997; Woodhouse, 2006):

$$l \propto r^{2/(3a)} \tag{1}$$

(where, l is stem length and r, radius), and (2) the length-to-radius constant of proportionality, m, so that

$$l = mr^{2/(3a)}. \tag{2}$$

This allometric formulation utilises biomechanical constraints that predict some optimal relationship between l and r. Decurrent trees (most broadleafed species) are appropriately described by the elastic similarity model, $a = 1$, whereas $a = 2/3$ represents geometric similitude with $l \propto r$, which (Niklas, 1994) reports is consistent with many observations of excurrent species (most conifers). Empirical data suggests that stems have often been better represented by some value greater than $a = 7/6$, similar to the case of stress similarity, a condition related to $a = 4/3$.

Here we focus on a range of values based on empirical studies and analysis of the radar backscatter modelling literature (Woodhouse, 2006) from $a = 2/3$ to $a = 4/3$, while recognising that some empirical results suggest that this scaling parameter may be larger (e.g. a mean of 1.81 in Zianis and Mencuccini (2004)). In the interests of space, we do not present all model results for differing

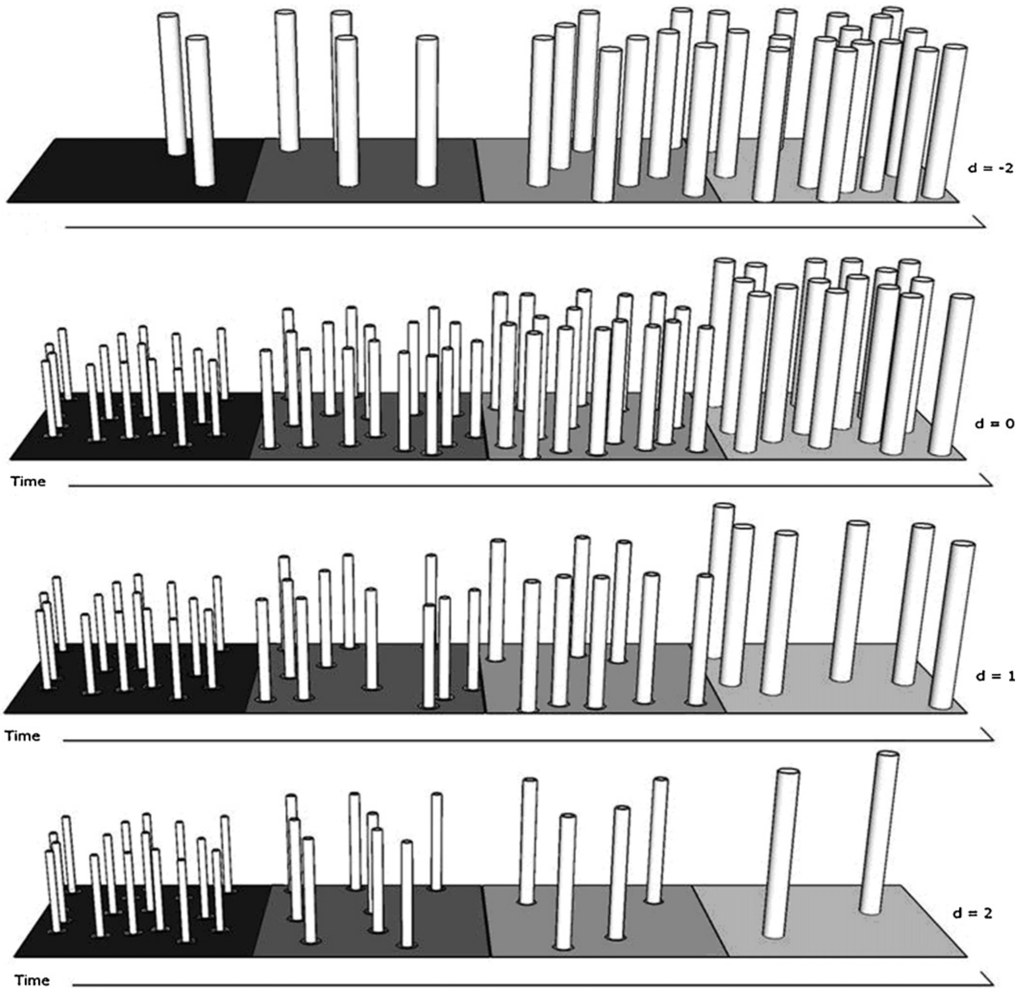

Fig. 1. Representation of collection of cylinders in five realistic forest settings. Area is schematic representation. From top to bottom $d = -2$, $d = 0$, $d = 1$ and $d = 2$ representing various thinning regimes over time. When d is positive the progression from left to right can represent a single stand changing over time or simply the state of four neighbouring plots at any time. When d is negative the progression cannot be considered with respect to time (and therefore stem growth) but is shown here with no stem size variation.

values of a, given that backscatter trends remain consistent, even if absolute values vary. Instead, we stick to a default choice of $a = 1$, representing the idealised "pipe" model in the branching model of West et al. (1997).

The constant of proportionality, m, is more diverse than observed values of a. Reported values range from approximately 5 to 163 in the dataset of Cannell (1982) which includes 675 forest communities. The default value in this study is chosen to be 20. We will show that while absolute values vary, the general trends remain similar for large variations of m.

2.2. Stem number densities (populations)

In radar measurements it is not usually possible to measure individual trees. The Matchstick Model therefore incorporates variability in both stem size, and stem number density. In the current work we only consider populations of identical stems so that variability of biomass per unit area is governed only by variability in size and number. This is a good representation of managed monocultures, but also a reasonable model for many single species forest areas. For forests of mixed size, this stem characterised in the model can be considered as a "representative" stem.

In any forest biome the number of trees of a given size is limited by the available resources and the balance between new growth and tree mortality (including herbivory and fire). These may vary both spatially and temporally. The relationship between the size (radius, r) and number of trees, N, can be characterised by a "thinning factor", d, such that

$$N \propto r^{-d}, \tag{3}$$

Although called a "thinning factor" it need not apply only to the change in a population over time (or a spatial surrogate, as in different aged managed stands) – we use it here as a general description of the size-number relationship. Fig. 1 visually describes the impact of d and demonstrates the relationship between size, number density and volume. When $d = 0, N$ is constant and total volume increases linearly with the volume of each stem. This is typical of young, actively growing forest (such as regeneration) where trees have yet to utilise all available resources, and tree mortality is near zero. Here, volume (biomass) per unit area will be positively correlated with N.

When $d = 2$, there is a dramatic decrease in N. The total volume still increases since the collective basal area remains constant (since each stem's basal area increases with r^2) while stem height increases. This is typical of many forests, especially in the tropics, or in managed forests where thinning has been applied in order to maintain basal area. It is exactly this dramatic change in structure associated with increasing area volume that the Matchstick Model tries to characterise (and is not incorporated into other simple single layer models). In this case the volume (biomass) per unit area is inversely proportional to N.

For $d = -2$, the increasing volume per unit area is positively correlated to N. This is typical of a resource-limiting case, such as savannas, whereby tree numbers are limited due to competition for scarce resources such as water, but where trees do grow they often need only grow to a sufficient height to outperform grasses and avoid fire and herbivory (Sankaran et al., 2008). This is shown in Fig. 1 by relating population increase without a corresponding individual radius increase to represent neighbouring plots.

To summarise, the thinning is directly related to the resources available per tree within an area and this in turn has an effect on the backscatter response. The amount of thinning directly affects forest number density and therefore backscatter (Champion et al., 1998). Changes in number density then have a significant effect on the space available for growth (Waring, 1983; Ginn et al., 1991) and with the growth of a tree determining the stem size and tree height it will have a direct influence on backscatter (Imhoff et al., 2001; Castel et al., 2002).

In the modelling results that follow, we look at different forests that begin with a finite number of small trees (the "planting density", p), which then grow and change in number, as given by N. We are then able to describe the impact of both d and p on the backscatter trends associated with increasing volume (and by implication, biomass). The range of basal areas and volume used within this study cover realistic values of up to 100 m^2/ha and 1000 m^3/ha respectively (Shula, 1989; Cannell, 1982), (Kinnunen et al., 2007). How volume, basal area and N change with d is illustrated in Fig. 2.

2.3. Scattering considerations

The simple model offered here considers the limiting case of cylinders with circumferences smaller than 0.1λ on the one hand, and larger than 10λ on the other. This corresponds to a relatively realistic range of circumferences for P-band (0.07–7 m), but less realistic at the high end for VHF (0.6–60 m). For the sake of simplicity, we refer to these limits as corresponding to "Rayleigh" and "Optical" scattering, respectively. In the Rayleigh case we assume the backscatter from each cylinder increases with the square of the cylinder volume, and for the latter, it increases with the physical cross-section (Kononov and Ka, 2008). At the transition between these two regimes lies resonant scattering, here we make an approximation that assumes the resonant behaviour "averages out" across this region due to the cumulative effect of a distribution of stem sizes. This assumption is supported by empirical results in Lopes et al. (1991), and Mougin et al. (1993), while Crispin Jr. and Maffett (1965) supports the Optical scattering simplification of the Mie scattering. This topic is considered more completely in Section 5.

Following the formulation by Smith and Ulander (2000) based on VHF backscatter from individual stems at polarisation p, we can write the radar cross section of a single tree stem as

$$\sigma_{PP} = \frac{4\pi}{L^2}\left| f_P(\theta)\frac{k^2(\varepsilon_r - 1)}{\pi(\varepsilon_r + 1)}\right|^2 V^2 \tag{4}$$

where V is stem volume, $f_P(\theta)$ is the Fresnel reflection coefficient of the surface, ε_r is the relative dielectric permittivity of the trunk, L is the attenuation, and k is the wavenumber. Given the simplicity of the Matchstick Model it is reasonable to consider all of these parameters, except V, to remain constant. The one point of discussion is whether it is an appropriate assumption for the attenuation, L. Smith and Ulander (2000) give a convincing case as to why this would be so at VHF wavelengths, but it is less clear whether this would be appropriate for, say, P-band. A compelling case for the importance of attenuation would normally be made based on evidence of saturation in the backscatter–biomass curves. However, it is just such an interpretation based on the Water Cloud model that we wish to challenge with the Matchstick Model. Indeed, the results presented in this paper demonstrate that the impact of thinning on the backscatter can be sufficient to cause saturation even when attenuation due to a thickening canopy and increasing number of scatterers is ignored. Saturation in itself is therefore not evidence of increasing attenuation by the forest layer.

In summary, we argue that we can characterise the trend in backscatter from each stem in the Matchstick Model as follows. For Rayleigh scattering:

$$\sigma_{Rayleigh} \propto V^2 \tag{5}$$

Using the relationship between length and radius of (1), the proportional relationship can then be written with respect to r and a as follows. The radar cross section per unit area is proportional to the cylinder volume:

$$\sigma^0_{Rayleigh} \propto N\, r^4 l^2 = N r^{(12a+4)/3a} \tag{6}$$

For Optical scattering, the normalised radar cross section scales with the physical cross-section:

$$\sigma^0_{optical} \propto N\, A = Nrl = Nr^{(3a+2)/3a} \tag{7}$$

This is in accordance with the laws of geometric optics, which under certain limitations is an acceptable simplification of the scattering formula for the physical optics of a cylinder. The physical optics formula for the radar cross section of a cylinder is shown below where k is the wavenumber, r the cylinder radius, l the cylinder length and θ represents the incident angle from broadside:

$$\sigma^0_{optical} = krl^2 \;\cos^2\theta \left[\frac{\sin(kl\,\sin\,\theta)}{kl\,\sin\,\theta}\right]^2 \tag{8}$$

By taking an average value over a symmetric window of incidence angles centred at $-\theta_w \le 0 \le \theta_w$ the average radar cross section of a cylinder becomes the integral:

$$\overline{\sigma^0_{optical}} = \frac{1}{\theta_w}\int_0^{\theta_w} krl^2 \;\cos^2\theta \left[\frac{\sin(kl\,\sin\,\theta)}{kl\,\sin\,\theta}\right]^2 d\theta \tag{9}$$

As this window approaches zero the small angle approximations of $\cos\theta = 1$ and $\sin\theta = 0$ apply, and following a change of variable and subsequent integration the formula reduces to a function of krl^2 to give the closed form formula for the average RCS of a cylinder around broadside, Eq. (10) (see also Hestilow, 2000):

$$\overline{\sigma^0_{optical}} = \frac{rl}{\theta_w}\left[Si(2kl\theta_w) - \frac{\sin^2(kl\theta_w)}{kl\theta_w}\right] \tag{10}$$

According to the rules of the sine integral function $Si(x)$, as the argument (x) approaches zero, $Si(x)$ will tend to x. Similarly by taking the limit of the angular window tending to zero we can rewrite Eq. (10) as below:

$$\begin{aligned}\overline{\sigma^0_{optical}} &= \lim_{\theta_w \to 0}\frac{rl}{\theta_w}\left[Si(2kl\theta_w) - \frac{\sin^2(kl\theta_w)}{kl\theta_w}\right]\\ &= \frac{rl}{\theta_w}\left[2kl\theta_w - kl\theta_w\right] = krl^2 \qquad (11)\end{aligned}$$

Where the window tends to zero and is approximately representative of the broadside angle the average radar cross section is proportional to the frequency and the cylinder volume. But in the limit of large arguments where $2kl\theta_w$ is large the function

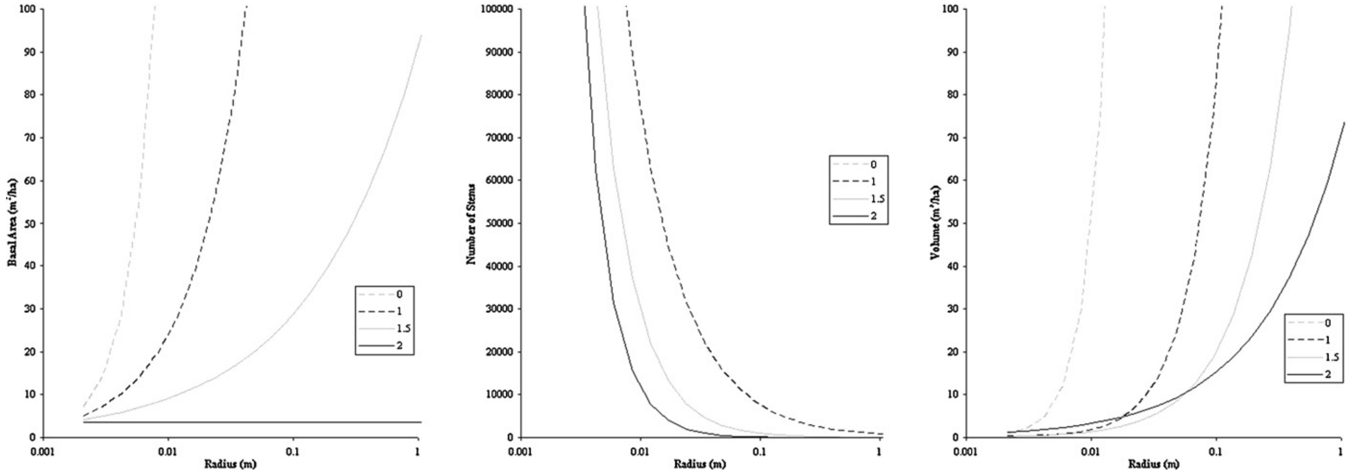

Fig. 2. Relationship of basal area (left), number of stems (centre), and volume (right) with respect to radius for varying thinning parameters representing identical forests starting from initial planting of 500,000. Legend represents *d* values of thinning parameter. Variations in *d* highlight how particular volumes and basal areas can be represented by different stem numbers and radii as a consequence of employed thinning.

$Si(\infty)\to\boldsymbol{\pi}/2$, and is known as the Dirichlet integral. Under the limits of $kl\theta_w$ tending to infinity (Eq. (12)) we can write the equation for average radar cross section of a cylinder as in Eq. (13):

$$\lim_{kl\theta_w\to\infty}\frac{\sin^2(kl\theta_w)}{kl\theta_w}\to 0 \tag{12}$$

$$\overline{\sigma^0_{optical}} = \frac{\pi rl}{2\theta_w} \tag{13}$$

This frequency invariant equation is then a function of the physical cross section of the cylinder in accordance with geometric optics. A full progression of the working is found in Hestilow (2000).

If the geometric optics is valid it can be stated that within P Band at 429 MHz the radius value of a scatterer coinciding with the transition from Rayleigh to Mie is about 0.01 m and the radius value of a scatterer which coincides with the transition from Mie to Optical is approximately 1.1 m, so cylinders greater than 2.2 m in diameter are deemed Optical scatterers for the purpose of this study.

An application of this simple approach is shown through the Matchstick Model data of Fig. 3, whereby the backscatter is shown as a logarithmic plot for 4 different planting densities in the absence of thinning ($d=0$). Two distinct phases are visible. The Rayleigh scattering is represented by the low biomass density data points, the region exhibiting a broad distribution among planting densities. The population density has a significant effect on the backscatter level in the Rayleigh. As the scattering transitions into Optical it is apparent that the relationship is less sensitive to the planting density. Note the similarities between the Matchstick Model representations of geometrical (Fig. 3 (left)) and physical optics (Fig. 3 (right)).

Regardless of polarisation the key trends remain the same with larger objects producing greater backscatter. HV backscattering is not the focus of the scattering behaviour in this study due to the absence of canopy scatterers to provide significant depolarising effects. The double bounce term involving the stem and ground is a significant component particularly at longer wavelength SAR, but the trend is still determined by the changing radar cross sections of the individual stems. For this reason the like polarised scenarios are chosen to highlight particular trends. Cross polarisation data shows identical trends to those reported in this study but at a much lower intensity level, highlighting the dominant effect of the double bounce mechanism at long wavelengths.

2.4. *Radiative transfer modelling using RT2*

RT2 is a multi-layer second order radiative transfer model similar to the MIMICS model used in Imhoff (1995b) and the UTACAN model used in Woodhouse and Hoekman (2000). It is described in Cookmartin et al. (2000) where it was used for modelling crop backscatter. In the current study, RT2 was used to investigate the backscatter from the Matchstick forest for a range of scenarios and is used for its accuracy in modelling backscatter trends rather than absolute values. RT2 is a fully polarimetric, second-order solution to the radiative transfer equations that treats vegetation canopy as a plane-stratified multilayer region over a rough surface. Its use in this instance is limited to a single plane with only vertical stems existing over a rough surface. The scattering properties of all plant components are derived from their depictions as simple geometric forms but here only plant stems are considered, represented as finite-length cylinders. Attenuation in RT2 is a function of branching layer penetration with the effects of occlusion in one layer carried over through transmission to the lower layer. As such possible effects of stem attenuation through occlusion are kept to a minimum as here only a single layer is used. Only in extremely dense planting scenarios do we believe this to have a significant impact on stem-ground interaction. These effects are investigated by modelling both at high and low planting densities as well as using different thinning rates to show that the impedance of the dihedral interaction between the stem and ground is not significant in the formation of saturation trends.

Within each RT2 calculation the backscatter for each polarisation is calculated. For this study the total backscatter is a combination of the direct and ground layer scattering from each layer, and the direct ground contribution. The ground composition is modelled using the model of Hallikainen et al. (1985) which requires a description of the soil in terms of sand, clay and silt. In addition a volumetric water content must be defined. Similar to the desired choice of low surface roughness throughout the modelling procedures the volumetric water content of the ground is also kept low to reduce the dielectric constant value and the influence of direct ground backscatter. As is shown in Hallikainen et al. (1985) a low value for volumetric water content can still produce a significant dielectric constant to allow scattering.

The backscatter values in relation to default RMS surface roughness and correlation length choices suggest that the ratio of these values is a defining aspect, as shown in Tang et al. (1996). Within the context of this work, the ratio of RMS surface roughness and

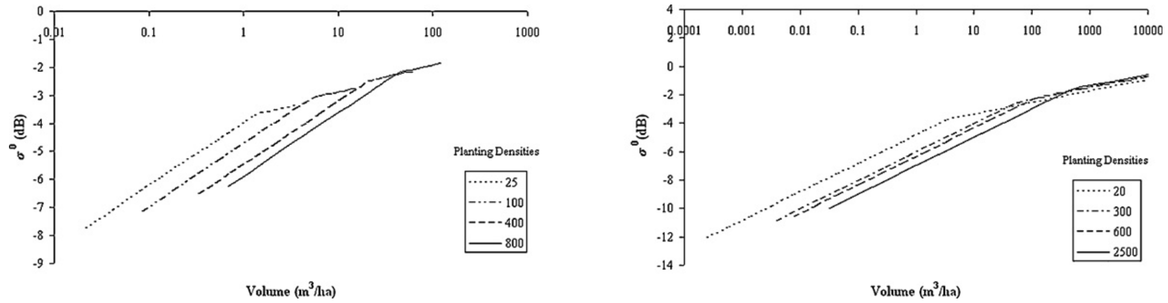

Fig. 3. Simple Matchstick Model predictions produced from varying planting densities. Data based on the combination of two equations representing the correlation of Optical backscatter with basal area, and the correlation of Rayleigh backscatter with the square of the volume. Planting densities vary in each figure and are chosen to achieve similar volume values. Figure on left represents geometric optics and on right physical optics. Note the similarity in trends.

correlation length is kept at a value indicating a rough surface. If a very rough surface is used the result will be that direct backscatter from the ground will dominate and render the forest less visible. Similarly, if a surface too smooth is used, the direct ground contribution will not be apparent due to dominance of specular reflection. The default ratio lies within the limits of validity, in accordance with Tang et al. (1996) with ground representations located at other locations within the range of validity producing almost identical results. Significantly for this study the trends remain the same regardless of the absolute backscatter values depicted, unless the surface is modelled as very rough.

3. Results: model data

Initial planting densities from 1 to 1×10^7 trees per hectare were used. This selection was made to encompass realistic planting densities as well as extreme cases which are less likely (for forest conditions) but allow realistic numbers later in the growing season. As well as the variation of planting density, the scaling is altered via the constant of proportionality m and scaling exponent a. Data has been modelled with RT2 for both VHF and P bands with attention paid primarily to the trends in backscatter rather than the absolute values.

Typical variations, due to changes in m, manifest as minute changes in trends, but show increased backscatter associated with longer stem lengths for similar radii.

In a similar fashion to the Matchstick Model predictions of Section 2.3, RT2 results (with zero thinning, as in Fig. 3) are shown in Fig. 4. The common feature regardless of planting density is the clustering of data points at higher volumes around a common trend in backscatter values. The low volumes in this figure are a consequence of the need to avoid extremely high basal areas resulting from higher initial planting densities in the absence of thinning.

3.1. Saturation effects

When a single stem is modelled (Fig. 5) it shows a trend change (even for very low stem volume) due to the transition to Optical scattering. The 50 MHz data shows similar trends but complete saturation would not be expected for a single stem exhibiting growth and increasing in size.

Data were modelled for sparse as well as dense (Fig. 6) stem scenarios with the backscatter values of each of these planting densities represented with respect to the radius. The trend is independent of planting density and scaling properties. In comparison with Fig. 6, Fig. 5 shows a single stem case that cannot undergo thinning. Although the trends with radius will not be the same for the single stem case the radius of transition remains the same showing that the transition is also independent of thinning.

The use of longer wavelengths in forest remote sensing has consistently been observed to move the point of backscatter saturation to higher biomass values (Table 1). This effect is normally attributed to decreasing opacity of the forest canopy as wavelength increases. For example, Smith and Ulander (1998) describe the theory of attenuation limitation as, "fundamentally linked with the high attenuation through the top of the foliage and the backscatter sensitivity to small-scale structures". When considering low numbers of single stems this attenuation is significantly reduced, and the large-scale structures (of the order of the wavelength) dominate the backscatter, yet the matchstick modelling still shows saturation occurring. Any saturation effects produced through modelling of solely stems, in concurrence with the Matchstick Model, is devoid of attenuation. This model therefore suggests that attenuation need not be the sole cause of saturation, but rather it is caused by a more complex issue related to stem radius, number density trends and wavelength. With regards to saturation, Table 1 expresses reported levels from empirical data in the literature.

3.2. The influence of stem radii on forest remote sensing using SAR

In the absence of thinning, the number density of a forest remains constant while lengths and basal areas becoming larger as a result of radii increase. Only the introduction of stem thinning will alter this. Individual backscatter from a stem is seen to vary for any particular volume for different constants of proportionality. This is primarily due to different length and radii combinations that make up these particular volumes. In order to concentrate on consistent stem-specific values, backscatter can be shown in terms of the radii of the stems (Figs. 7 and 8).

The transition point between the theorised Mie scattering regime and the Optical and Rayleigh scattering regimes appear to be an accurate representation as to when the saturation process occurs, signifying a clear dependence on radius. General trends appear to be independent of the constant of proportionality and saturation is only dependent on the scattering change from Rayleigh to Mie, through the dependence on stem radius. Increasing the constant of proportionality increases the level of backscatter but does not substantially alter the trend.

4. Results: saturation

4.1. Initial findings

Modelling has shown that saturation can theoretically be caused by a change in scattering regime and so is influenced by factors such as radius, and length. This may serve as an additional or alternative explanation to that proposed by occlusion. Saturation is generally associated with the rapid decrease in the rate of change of backscatter with increasing stem volume, and therefore biomass density.

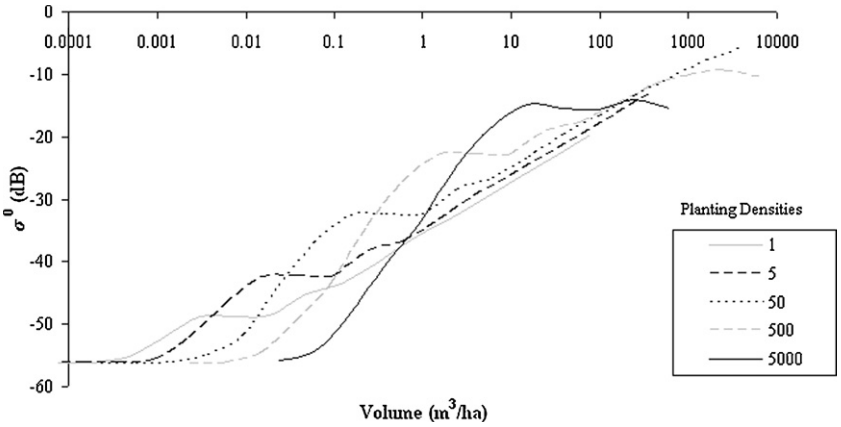

Fig. 4. VV P Band data for multiple planting densities in the absence of thinning, modelled using RT2. Number densities are maintained at the planting density level for duration of growth signifying zero mortality.

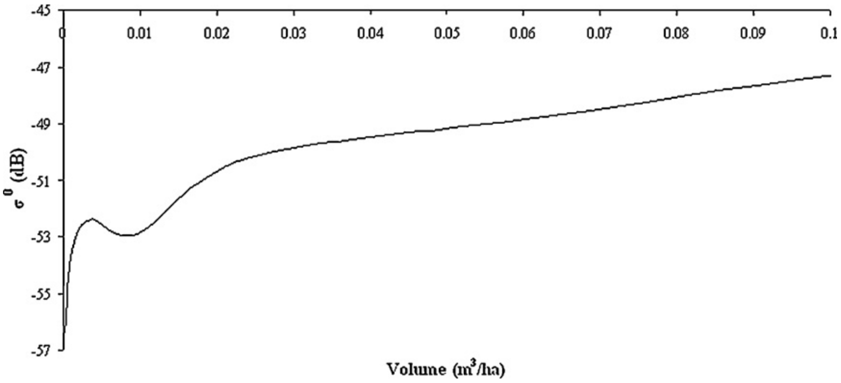

Fig. 5. Single stem P Band VV backscatter when constant of proportionality in scaling $m = 10$ in the absence of thinning. Transition effects evident through change in backscatter trend.

The following modelling procedures serve to provide an explanation as to the existence of this effect using the application of a thinning factor d introduced in Woodhouse (2006). The majority of modelling presented so far in this work has assumed a thinning factor of 0. This assumes that no thinning takes place within the forest, signifying perpetual growth. This scenario, as it sounds, is unnatural due to the limited resources available to a forest, the main factor behind natural thinning processes. In addition, managed thinning is a procedure used in managed plantations as a means of achieving maximum useable wood from a particular species. For biomass retrieval schemes the effects of thinning are an important aspect that must be taken into account (Castel et al., 2002).

The main effect of introducing a thinning factor to forest modelling is the direct change in basal area resulting from a loss of stems while growth in the remaining stems continues. As the height of the stems increase with each increment, the forest volume is still expected to increase, with the notion that fewer larger stems will contain a greater volume than several smaller stems (Fig. 1).

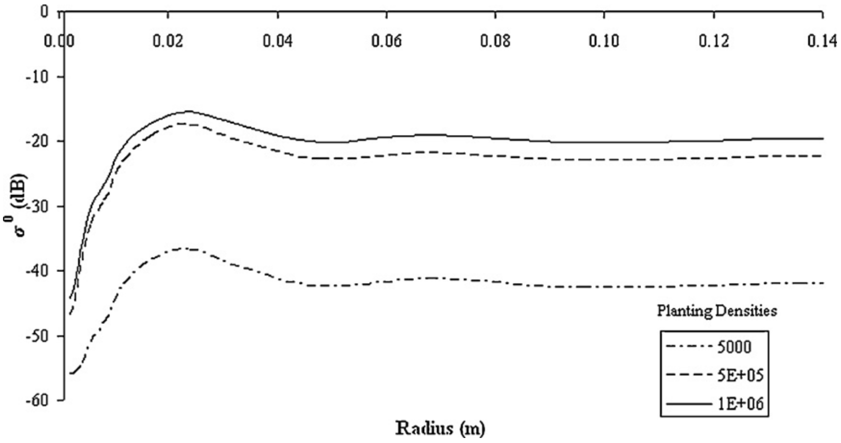

Fig. 6. RT2 data for P-band VV with $d = 2$ thinning. As stem radii increase, total backscatter increases until radii are large enough to make the transition to Optical scattering, where the backscatter increase is balanced out by the number density decrease. Legend shows planting densities prior to thinning effects which reduce the numbers significantly at each growth increment. For example for the 1 million planting density there are 244 stems when the radius equals 0.1 m.

Table 1
SAR observed "saturation" limits (Patenaude et al., 2005).

SAR biomass saturation values	Acquisition	Frequency	Biomass density (B) or volume (V) saturation	Sources
Northern Conifers, France	Airborne Backscatter amplitude	P-band, L-band	B: 200 t ha^{-1} B: 100 t ha^{-1}	Dobson et al. (1992)
Northern Michigan	Orbital Polarimetric and modelling	C-Band (SIR), X-Band (SIR)	B: 250 t ha^{-1}	Dobson et al. (1995)
Boreal Conifer, Sweden	Satellite Backscatter amplitude	C-Band (ERS-1), L-Band (JERS-1)	V: 64 m^3/ha V: 143 m^3/ha	Fransson and Israelsson (1999)
Norway spruce, Sweden	Airborne Backscatter amplitude	VHF	No volume Saturation	Fransson et al. (2000b)
Coniferous Europe and North America.	Airborne Backscatter amplitude	P-Band L-Band C-band	B: 100 t ha^{-1} B: 40 t ha^{-1} B: 20 t ha^{-1}	Imhoff (1995a)
Tropical	Satellite Interferometric coherence	L-Band (JERS)	B: 60 t ha^{-1}	Luckman et al. (1998)
Boreal, Canada	Satellite Multifrequency and polarisation	C-band (SIR)X-band (SIR)L-band	B: 200 t ha^{-1} ratio between L-band HH and C-Band HV	Ranson et al. (1995)
Northern Maine	Airborne Multifrequency and polarisation	L-band, P-band	B: 150 t ha^{-1} (using HV polarisation)	Ranson and Sun (1994)
Tropical transition region Cameroon	Satellite Backscatter, polarisation (HH/HV)	L-band (JERS-1, ALOS PALSAR)	100–150 Mg ha^{-1} biomass (JERS-1, HH), 150–200 Mg ha^{-1} (ALOS PALSAR, HV)	Mitchard et al. (2011)
Tropical savanna, woodland and forest/savanna Cameroon, Uganda, Mozambique	Satellite Backscatter, polarisation (HH/HV)	L-band (ALOS PALSAR)	No real prediction accuracy above 200 Mg ha^{-1}	Mitchard et al. (2009)

In the case of thinning being equal to 2, the total basal area of a plot of stems will remain constant, so that as the stems increase their individual basal areas, the number of stems must reduce. The backscatter is dependent on the number of stems and the basal area of each individual stem. Thinning is related to the radial increases in the stem through the equation:

$$N = r_k^{-d} \cdot r_0^{d} \cdot pdens \tag{14}$$

where *pdens* represents the initial planting density of stems and subscript k represents an incremental increase in radius from the initial value associated with r_0.

Between the values $d = 0$ to 2 the rate of change of backscatter with volume is expected to reduce. According to the simple Matchstick Model, when $d = 2$, the backscatter signal will saturate in the Optical region. When d is not equal to this value the basal area will continue to increase or decrease with a continued increase in backscatter (Fig. 9a and b). The basal areas featured are higher than typical basal areas but were chosen to allow the use of more data points and enable closer comparison between different thinning levels.

For $d = 2$ thinning, the number of stems will reduce with each size increment but collective volume will increase as remaining stems become taller and thicker. As a result, backscatter will continue to increase within the Rayleigh regime and show a distinct correlation between the backscatter and the volume. Through the Optical regime backscatter will remain constant. As Optical backscatter is directly related to the area of individual stems multiplied by the number present, or in essence total basal area, then zero basal area increase indicates zero backscatter increase manifesting in a zero gradient. For a forest containing stems increasing in size according to the scaling exponent $a = 2/3$, Eq. (13) defines that the Optical backscatter will be directly proportional to the square of the radius when combined with Eq. (2). This proportionality links the basal area directly with the backscatter.

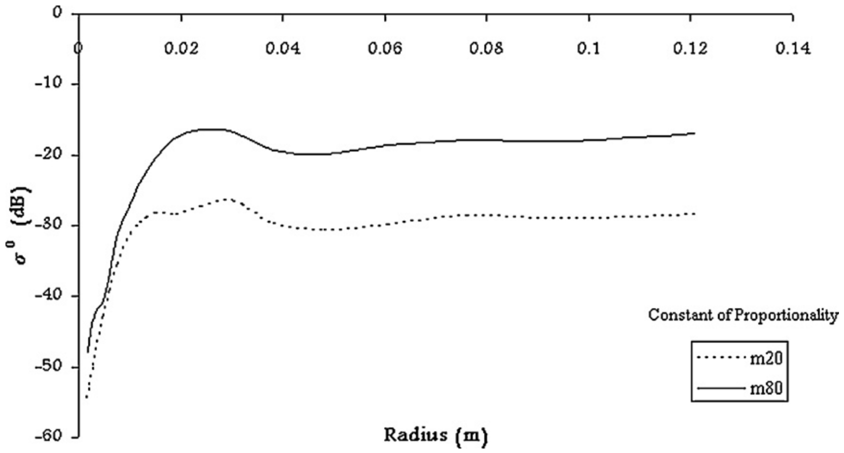

Fig. 7. P Band VV data for initial planting density of 5×10^5 stems with thinning parameter of $d = 2$. The two lines show different values of m the scaling constant of proportionality. In both cases, the scaling exponent $a = 2/3$ and exhibit classic "saturation" behaviour due to the increasing radii of stems.

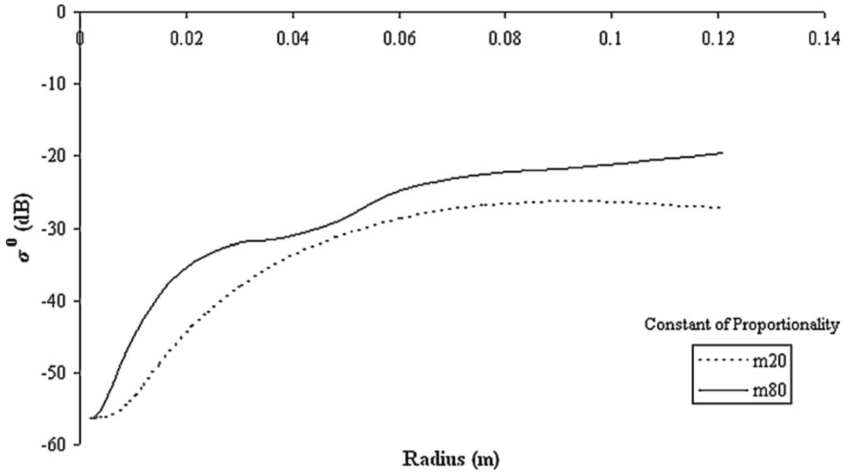

Fig. 8. VHF Band VV data for initial planting density of 5×10^5 stems with thinning parameter $d = 2$. The two lines show different values of m the scaling constant of proportionality. In both cases, the scaling exponent $a = 2/3$. Both cases exhibit classic "saturation" behaviour due to increasing radii of stems. The constant of proportionality does little to affect the general curve shape.

Modelling to visualise these scenarios, using RT2, was performed on data featuring variations in the thinning exponent, d. The constant of proportionality m, and the initial planting density were also varied. These variations provide a broad analysis of possible stem structures produced by nature and allow comparison with the simplistic Matchstick Model (Fig. 9a and b). The modelling explored volumes up to and beyond noted values. These values of volume are far higher than featured saturation values in empirical

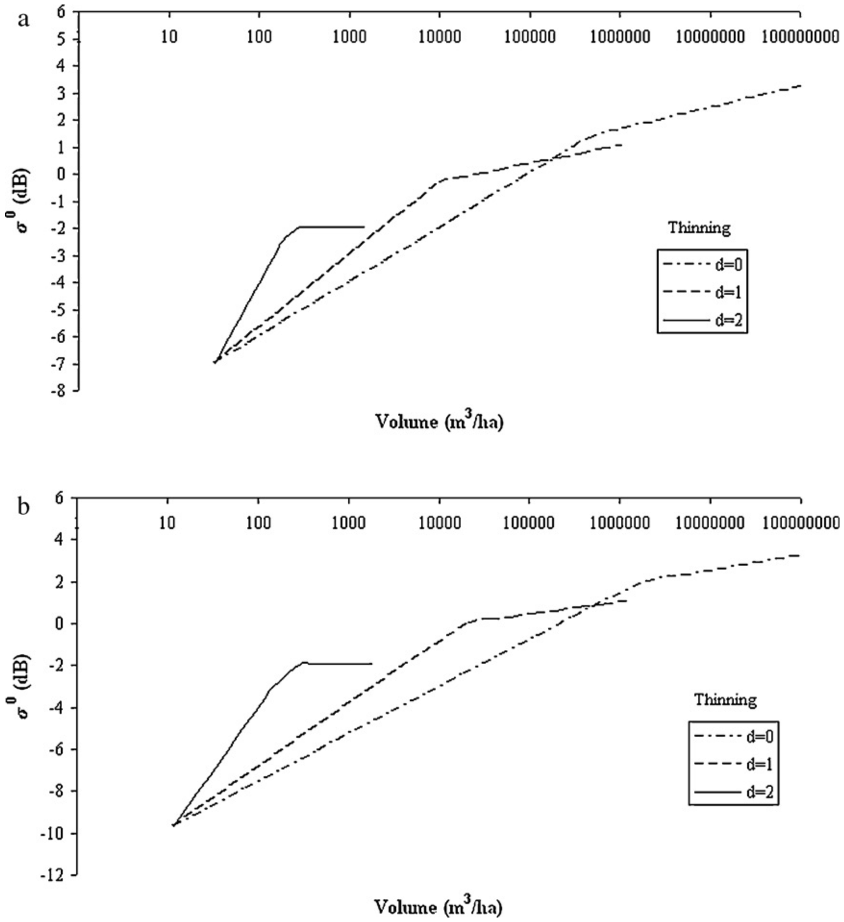

Fig. 9. (a) Matchstick Model representation using physical optics of P-Band backscatter associated with thinning. $d = 2$ shows constant total basal area at 35 m^2/ha as forest volume increases, $d = 0$ shows increasing basal area from initial 35 m^2/ha, and $d = 1$ shows increasing basal area from 35 m^2/ha. Initial planting density 2.5E06. Note that $d = 2$ exhibits the classic saturation shape while $d = 0$ thinning reaches excessive volume values not intended to be representative of natural forests but to highlight trends. (b) Matchstick Model representation using geometric optics of P-Band backscatter associated with thinning. $d = 2$ shows constant total basal area at 35 m^2/ha as forest volume increases, $d = 0$ shows increasing basal area from initial 35 m^2/ha, and $d = 1$ shows increasing basal area from 35 m^2/ha. Initial planting density 2.5E06. Note that $d = 2$ exhibits the classic saturation shape while $d = 0$ thinning reaches excessive volume values not intended to be representative of natural forests but to highlight trends.

studies (Table 1). Through modelling, when a thinning factor of $d = 2$ is applied, saturation occurs, whereas when $d = 1.5$ a change in the gradient of the backscatter–volume trend line is seen but not saturation. If this modelling is correct then the existence of saturation, even at VHF band, is not entirely dependent on the volume present but also on the forest thinning and in turn the change in total basal area and stem numbers. According to physical laws, Eq. (7), in the absence of significant attenuation and with increasing basal area, backscatter will increase. The gradient of increase within the Mie and Optical regimes will be greater for a $d = 1$ than a $d = 2$ forest. The transition between Rayleigh and Optical scattering therefore becomes less significant when plotting backscatter against biomass density at low thinning values up to reasonable volume limits.

When full trees are considered in a natural forest, the canopy will at some point reach a level where it will remain constant as stems continue to grow. According to empirical studies at 429 MHz (Table 1), at a biomass density in the region of 100–200 t ha^{-1}, it is expected that saturation will take place. This theory then suggests that the cross-sectional area of a collection of similar sized branches may have a constant total cross-sectional area, which would scatter optically. As the smaller branches will scatter optically at a smaller wavelength, saturation for these frequencies will therefore occur at lower biomass values offering an additional explanation why saturation at higher frequencies occurs at lower biomass densities. Figs. 10 and 11 show how the saturation volume varies with thinning and may not correspond with planting density for both VHF and P Bands respectively.

In addition to these observations, it is noticeable that the 429 MHz datasets show evidence of oscillation at volumes associated with saturation with an average over this range required to show gradient variations associated with thinning. These oscillations could relate to the Mie oscillatory trends existing between Rayleigh and Optical scattering and should not be disregarded without consideration.

5. Mie oscillations

In order to investigate the possibility of Mie oscillations in the region of saturation the modelling procedures were altered. Originally every backscatter value was associated with a volume determined from a collection of identical stems whose number at any particular point was controlled by initial planting density and thinning factor. It is thought by changing this depiction to something slightly more realistic, any oscillations will be minimised. To increase the realism, a series of randomly generated stems were used. The stems were chosen to possess radii values within one standard deviation of the mean. In essence this variation transforms a mono-sized forest into a multi-sized forest, in keeping with natural forest growth.

Under the new conditions of modelling, the thinning factor was maintained at a value of $d = 2$ and an initial planting density of 10×10^6 was used, a significantly high value due to the large thinning effect of $d = 2$ with each increment. These parameters would allow an approximately constant basal area over the test site and allow a reasonable value of volume at all stages of the forest growth through each radius increment representative of natural settings with initial increments resulting in high mortality.

Modelling the forest in this new way allows comparison of forests consisting of: (1) mono sized vertical stems, (2) multi-size, vertical stems, (3) mono size, non-vertical stems and (4) multi-size, non-vertical stems (Figs. 12 and 13). By modelling these alternate forest structures while maintaining the Matchstick Model ethic it can also be determined whether the mono and vertical nature of the stems at each volume increment have any bearing on the presence of Mie oscillations and in effect the backscatter. In the presence of a single object, Mie oscillations would be expected, and it is assumed that the same behaviour, to some extent, is exhibited with a collection of identical stems. As such these oscillations are not generally seen or noted in empirical data possibly due to the large stem numbers present and their variable sizes.

At 35 degrees incidence the data appears largely unaffected by Mie oscillations. At both 50 MHz and 429 MHz the same trends are apparent with higher backscatter in general for non-vertical stems at VV but lower for HH as a result of stronger double bounce contribution. When non-vertical stems are modelled there is little difference in backscatter whether the stems are homogeneously or heterogeneously sized. This is apparent when modelling vertical stems, despite the identical trends existing between the two datasets. When these scenarios are modelled at lower incidence angles oscillations are evident in the mono sized stems alone, this oscillatory behaviour at lower incidences is removed by varying the size distribution of the stems but also by introducing non-vertical stems of random angles over a spherical distribution. At 35 degrees incidence these oscillations are not evident.

Introducing non-vertical stems appears to remove the oscillations at volumes consistent with Mie scattering at low incidence angles without an effect on the Rayleigh region. In a natural forest setting, in a climax forest, stems will appear to be very similar in size but not identical. The stems which appear very similar in size are more accurately described using a distribution about a mean value. Empirical SAR backscatter values can be extremely variable in terms of correlation with volume. It is for this reason that these datasets are shown, highlighting the effect on backscatter that verticality and size distribution have on the resultant backscatter. Within the Matchstick Model set up, the stem sizes could be less constrained and yet still provide sensible correlation with the backscatter to coincide with more natural settings. The negative trends in the data following saturation could be construed as a result of the presence of non-vertical stems over such great an angular range. Saturation does not appear to be affected by the parameters varied here but backscatter intensity is significantly influenced by the size distribution and orientation of stems.

6. Discussion

SAR backscatter has been shown to correlate empirically with the standing biomass density of forests (Karam et al., 1993), yet robust generic relationships have remained elusive. The correlation is often thought to be dependent on the incident SAR wavelength and the volume of the forest – RVoG or Water Cloud Model explains these trends as the increasing volume of vegetation resulting in increasing backscatter, and saturation caused by the increasing forest opacity. The significance of the Matchstick Model presented here is that it challenges those models and provides an alternative explanation by considering macroecological trends in forest stem size and number density that determine the consolidation of the biomass material, which has been previously shown to impact on backscatter (Imhoff, 1995b; Woodhouse, 2006; Dobson et al., 1995). Saturation need not only be caused by increased opacity, but rather, by the physical structure of the forest as it moves from low biomass to high biomass, including the changes in stem number densities.

When structure (i.e., size and number density) is highly correlated with biomass, the backscatter – biomass trend also has a strong correlation. However, such structural trends are highly varied in nature – in some areas biomass is positively correlated with size and number density, while in others it is positively correlated with size but negatively correlated with stem density. When backscatter is modelled across a variety of realistic radii, basal areas and number densities, the result has no clear trend (Fig. 14). If backscatter is not a robust measure of biomass even for a simple

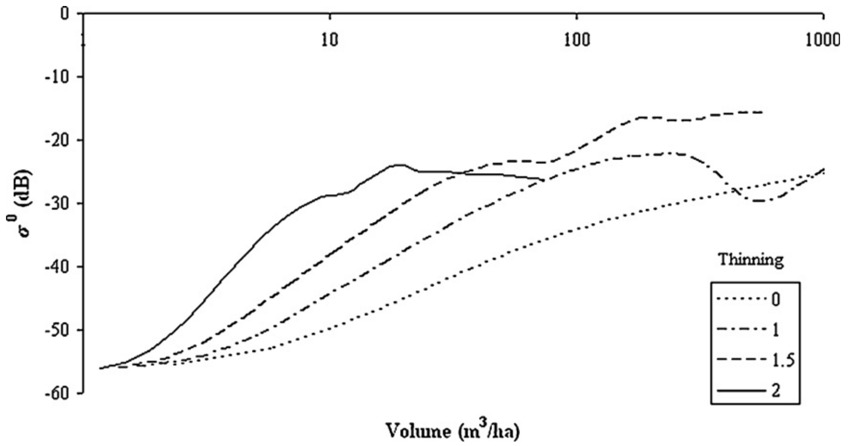

Fig. 10. RT2 modelling backscatter results for VHF Band VV incident waves of 50 MHz frequency on a forest of initial planting density of 5×10^5 stems undertaking different thinning regimes.

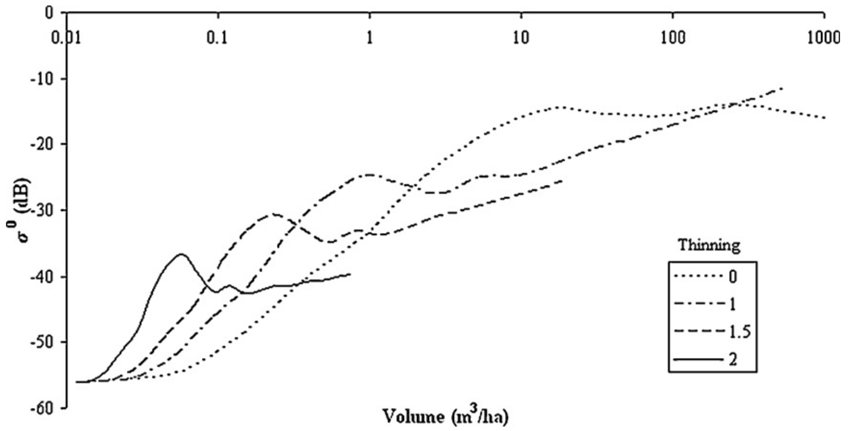

Fig. 11. RT2 modelling results for P Band VV incident waves on initial planting density of 5×10^3 stems per ha. when thinning regime is varied between $d = 0$ and $d = 2$. Note that the classic "saturation" curve occurs at thinning rates closest to $d = 2$ which maintains a constant basal area. All values less than $d = 2$ produce trends that remain positive, polarisation chosen to emphasise trends.

single layer Matchstick Model, then we must urge great caution when trying to apply generic trends across different forest biomes. The important conclusion is that backscatter does not measure biomass, but measures structural trends that are correlated with biomass in different ways, driven by stand level competition, resource use, etc. As a result different forest growth regimes should expect different backscatter–biomass trends.

In this respect, VHF does not avoid interrogation. With regards to 50 MHz data the transition from Mie to Optical scattering is believed to occur at radii of approximately 9.54 m. Trees of this size do not occur in nature (General Sherman has a diameter of 11 m) and as a result complete saturation would not necessarily be expected in empirical data when using this wavelength. However, the modelled results presented here also establish that

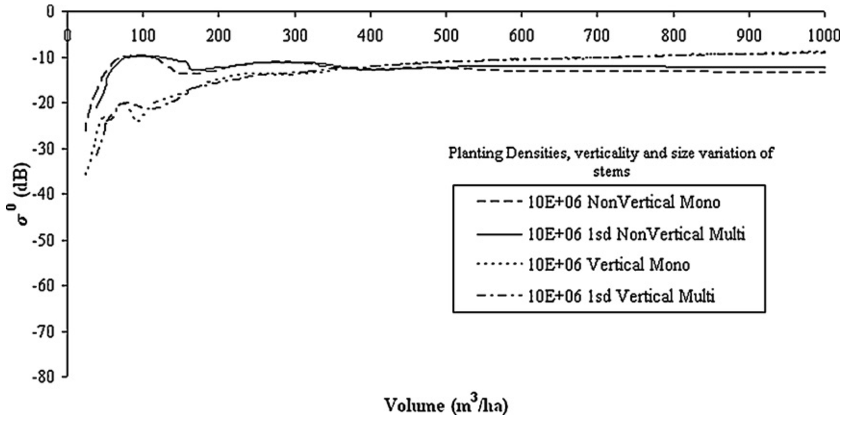

Fig. 12. VV P Band data of 429 MHz for initial forest planting density of 10×10^6 stems with thinning $d = 2$, featuring vertical and non-vertical stem variations of multi and mono radii forests. Saturation seen in presence of approximately 1220 stems at 373 m^3/ha for vertical stems. Note number density reduces significantly with every size increment as volume increases. Polarisation chosen to emphasise trends.

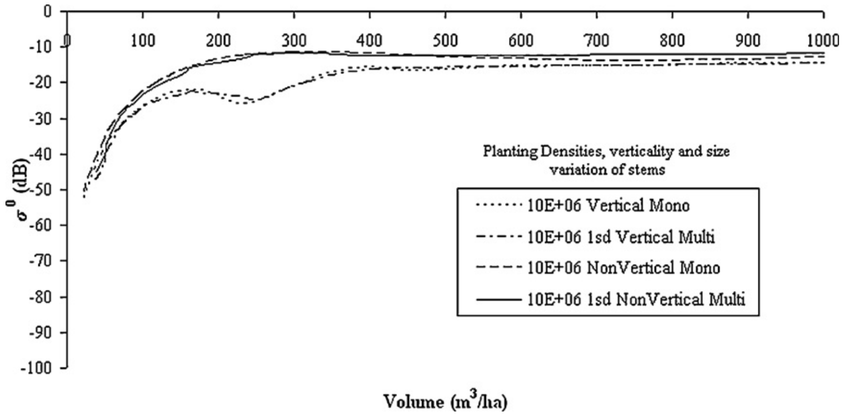

Fig. 13. VV VHF Band data of 50 MHz for initial forest planting density of 10×10^6 stems with thinning $d = 2$, featuring vertical and non-vertical stem variations of multi and mono radii forests. Saturation seen in presence of approximately 610 vertical stems at 417 m^3/ha. Note number density reduces significantly with every size increment as volume increases. Polarisation chosen to emphasise trends.

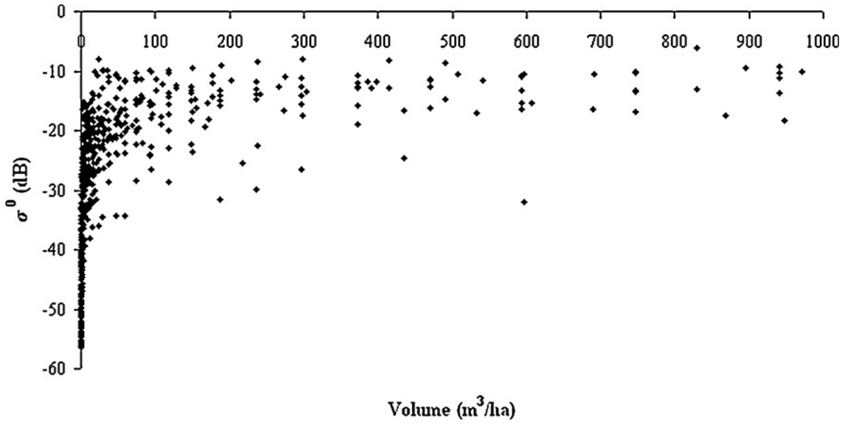

Fig. 14. VV polarised P Band backscatter values for various planting densities, thinning components, scaling parameters, and constants of proportionality at 429 MHz. Similar trends exist for VHF data. The non-uniqueness of backscatter to volume relationship is apparent. Low volume data is included although such low volume values may only be present in modelled data.

robust trends are not possible with VHF when averaging backscatter over many stems. CARABAS (Smith, 2000) demonstrates such consistently good results because they resolve individual trees and thinning rates are irrelevant.

We have shown here that complete saturation occurs when the value of the thinning parameter is set at $d = 2$. This value is in accordance with thinning rates recorded in macroecology (Enquist and Niklas, 2001) which here correspond to a constant forest basal area. Thinning parameter values higher than 2 correspond to rates of stem mortality beyond those expected for competitive behaviour alone (Coomes et al., 2003) while according to Eq. (3) a value of 0 corresponds to zero thinning. It is accepted by the authors that saturation may occur at different values around this value as thinning in nature may not be the same in any given situation. What is apparent in the Matchstick Model simulations is that relative variations of this thinning value above and below the $d = 2$ value can provide data that appears relatively saturated as well as the possibility of providing a diminishing backscatter return when exceeded.

From a macroecological perspective, the addition of smaller branches to each stem in the model will not affect the overall trend as backscatter is still governed by thinning rates. The relative contribution of backscatter through the canopy from different sized cylinders as wavelength is increased is shown in Brolly and Woodhouse (2012). The increasing contribution from the larger objects at the longer wavelengths is justification for the emphasis placed on long wavelength SAR interactions with stems in this work. In addition evidence is provided by empirical studies which have highlighted the significance of stem-ground double bounce mechanisms at these wavelengths such as those exhibited at P (Saatchi and McDonald, 2002) and VHF (Fransson et al., 2000a; Hallberg et al., 2005) bands.

7. Conclusions

We have introduced the “Matchstick Model” as a new deductive approach to modelling backscatter from a forest. As the majority of a forest's biomass is concentrated in the stems it would seem reasonable to remove all but the stems from the modelled forest and consider this a realistic representation of natural biomass distribution when considering long wavelength SAR. Although we consider a forest devoid of canopy and branches it is not unrealistic to assume that this is an adequate representation of the scenario experienced for SAR forest remote sensing. As the incident wavelength is increased the scenario exists where only the largest targets will show sensitivity. This is very similar to the case with VHF SAR while the significance of the stem contribution to the backscatter through the double bounce mechanism at P-Band has been previously reported (Saatchi and McDonald, 1997). The reader is also referred to Brolly and Woodhouse (2012) which emphasises the significance of larger scattering objects within the vertical forest structure as the incident wavelength is increased.

The “Matchstick Model” predicts that SAR forest backscatter saturation can be caused by tree stem scattering going from one scattering regime to another, combined with a stem thinning rate. These transitions produce two distinct phases in backscatter with regards to a forest increasing in volume. The model explains why a robust and consistent backscatter–biomass trend has been so elusive–because forests accumulate biomass in different ways, and these differences have profound influence on the backscatter, even in very simple cases. Although the "Matchstick Model" has been designed to model biomass distribution in a more ecologically accurate scenario than scattering models such as WCM and RVOG, it must not be assumed that the lack of correlation between backscatter and biomass contradicts the nature of the model. For example, take, in extremis, VHF where only modelling of the backscatter from the stems is required due to the wavelength size. Modelling the stems then incorporates structural information that governs 90% of the biomass. However, the resulting backscatter (when backscatter from more than one tree is measured at a time) is not well correlated with biomass, unless the thinning rates are also well-correlated. Backscatter and its trends are sensitive to a combination of biomass *and* its distribution. The "Matchstick Model" aims to incorporate both elements.

The model reinforces the risk of not considering forest structure when using backscatter as an indicator of biomass, and is a word of warning for possible future satellite instruments. This work builds a foundation in which to explore how to account for variability in planting densities and thinning rates, and this will form the focus of future studies.

Role of the funding source

Funding for this study was provided by the Natural Earth Research Council (NERC) of the United Kingdom.

References

Attema, E.P.W., Ulaby, F.T., 1978. Vegetation modeled as a water cloud (for radar sensing of crops). Radio Science 13, 357–364.

Bastien-Henri, S., Park, A., Ashton, M., Messier, C., 2010. Biomass distribution among tropical tree species grown under differing regional climates. Forest Ecology and Management 260, 403–410.

Brolly, M., Woodhouse, I.H., 2012. Vertical backscatter profile of forests predicted by a macroecological plant model. International Journal of Remote Sensing, TRES-PAP-2011-0454.R1, in press.

Bush, T., Ulaby, F., 1976. Radar return from a continuous vegetation canopy. IEEE Transactions on Antennas and Propagation 24, 269–276.

Cannell, M.G.R., 1982. World Forest Biomass and Primary Production Data. Academic Press, New York.

Castel, T., Guerra, F., Caraglio, Y., Houllier, F., 2002. Retrieval biomass of a large Venezuelan pine plantation using JERS-1 SAR data. Analysis of forest structure impact on radar signature. Remote Sensing of Environment 79, 30–41.

Champion, I., Guyon, D., Riom, J., Toan, T.L., Beaudoin, A., 1998. Effect of forest thinning on the radar backscattering coefficient at L-band. International Journal of Remote Sensing 19, 2233–2238.

Cookmartin, G., Saich, P., Quegan, S., Cordey, R., Burgess-Allen, P., Sowter, A., 2000. Modeling microwave interactions with crops and comparison with ERS-2 SAR observations. IEEE Transactions on Geoscience and Remote Sensing 38, 658–670.

Coomes, D.A., Duncan, R.P., Allen, R.B., Truscott, J., 2003. Disturbances prevent stem size density distributions in natural forests from following scaling relationships. Ecology Letters 6, 980–989.

Crispin Jr., J.W., Maffett, A.L., 1965. Radar cross-section estimation for simple shapes. Proceedings of the IEEE 53, 833–848.

Dobson, M.C., Ulaby, F.T., LeToan, T., Beaudoin, A., Kasischke, E.S., Christensen, N., 1992. Dependence of radar backscatter on coniferous forest biomass. IEEE Transactions on Geoscience and Remote Sensing 30, 412–415.

Dobson, M.C., Ulaby, F.T., Pierce, L.E., Sharik, T.L., Bergen, K.M., Kellndorfer, J., Kendra, J.R., Li, E., Lin, Y.C., Nashashibi, A., 1995. Estimation of forest biophysical characteristics in Northern Michigan with SIR-C/X-SAR. IEEE Transactions on Geoscience and Remote Sensing 33, 877–895.

Enquist, B.J., Niklas, K.J., 2001. Invariant scaling relations across tree-dominated communities. Nature 410, 655–660.

Fang, J., Wang, G.G., Liu, G., Xu, S., 1998. Forest biomass of China: an estimate based on the biomass–volume relationship. Ecological Applications 8, 1084–1091.

Fransson, J.E.S., Gustavsson, A., Ulander, L.M.H., Walter, F., 2000a. Towards an operational use of VHF SAR data for forest mapping and forest management. In: Proceedings 2000 IEEE International Geoscience and Remote Sensing Symposium, IGARSS'04, 1, pp. 399–401.

Fransson, J.E.S., Israelsson, H., 1999. Estimation of stem volume in boreal forests using ERS-1 C-and JERS-1 L-band SAR data. International Journal of Remote Sensing 20, 123–137.

Fransson, J.E.S., Smith, G., Walter, F., Gustavsson, A., Ulander, L.M.H., 2004. Estimation of forest stem volume in sloping terrain using CARABAS-II VHF SAR data. Canadian Journal of Remote Sensing 30, 651–660.

Fransson, J.E.S., Walter, F., Ulander, L.M.H., 2000b. Estimation of forest parameters using CARABAS-II VHF SAR data. IEEE Transactions on Geoscience and Remote Sensing 38, 720–727.

Gibbs, H.K., Brown, S., Niles, J.O., Foley, J.A., 2007. Monitoring and estimating tropical forest carbon stocks: making REDD a reality. Environmental Research Letters 2, 045023.

Ginn, S.E., Seiler, J.R., Cazell, B.H., Kreh, R.E., 1991. Physiological and growth responses of eight-year-old loblolly pine stands to thinning. Forest Science 37, 1030–1040.

Hallberg, B., Smith-Jonforsen, G., Ulander, L., 2005. Measurements on individual trees using multiple VHF SAR images. IEEE Transactions on Geoscience and Remote Sensing 43, 2261–2269.

Hallikainen, M.T., Ulaby, F.T., Dobson, M.C., El-Rayes, M.A., Wu, L.K., 1985. Microwave dielectric behavior of wet soil—part 1: empirical models and experimental observations. IEEE Transactions on Geoscience and Remote Sensing, 25–34.

Hestilow, T.J., 2000. Simple formulas for the calculation of the average physical optics RCS of a cylinder and a flat plate over a symmetric window around broadside. IEEE Antennas & Propagation Magazine 42, 48–52.

Imhoff, M.L., 1995a. Radar backscatter and biomass saturation: ramifications for global biomass inventory. IEEE Transactions on Geoscience and Remote Sensing 33, 511–518.

Imhoff, M.L., 1995b. A theoretical analysis of the effect of forest structure on synthetic aperture radar backscatter and the remote sensing of biomass. IEEE Transactions on Geoscience and Remote Sensing 33, 341–352.

Imhoff, M.L., Johnson, P., Carson, S., Lawrence, W., Condit, R., Stutzer, D., Wright, J., 2001. VHF radar mapping of forest biomass in Panama. In: IEEE 2001 International Geoscience and Remote Sensing Symposium, IGARSS'01, p. 1.

Karam, M.A., LeVine, D.M., Amar, F., Fung, A.K., Mougin, E., Lopes, A., 1993. Understanding the relation between the forest biomass and the radar backscattered signals. In: International Geoscience and Remote Sensing Symposium. Better Understanding of Earth Environment, Tokyo, Japan, pp. 573–575.

Kinnunen, J., Maltamo, M., Paivinen, R., 2007. Standing volume estimates of forests in Russia: how accurate is the published data? Forestry 80, 53.

Kononov, A.A., Ka, M.H., 2008. Model-associated forest parameter retrieval using VHF SAR data at the individual tree level. IEEE Transactions on Geoscience and Remote Sensing 46, 69–84.

Le Toan, T., Beaudoin, A., Riom, J., Guyon, D., 2002. Relating forest biomass to SAR data. IEEE Transactions on Geoscience and Remote Sensing 30, 403–411.

Lopes, A., Mougin, E., Beaudoin, A., Karam, M.A., 1991. Relating the microwave signatures of trees to their structure results of an experimental/theoretical approach. In: 1991 International Geoscience and Remote Sensing Symposium. Remote Sensing: Global Monitoring for Earth Management, IGARSS'91, p. 1.

Luckman, A., Baker, J., Honzak, M., Lucas, R., 1998. Tropical forest biomass density estimation using JERS-1 SAR: seasonal variation, confidence limits, and application to image mosaics. Remote Sensing of Environment 63, 126–139.

Mette, T., Papathanassiou, K., Hajnsek, I., 2004. Biomass estimation from polarimetric SAR interferometry over heterogeneous forest terrain. In: Proceedings 2004 IEEE International Geoscience and Remote Sensing Symposium, IGARSS'04, p. 1.

Mitchard, E., Saatchi, S., Lewis, S., Feldpausch, T., Woodhouse, I., Sonké, B., Rowland, C., Meir, P., 2011. Measuring biomass changes due to woody encroachment and deforestation/degradation in a forest-savanna boundary region of central Africa using multi-temporal L-band radar backscatter. Remote Sensing of Environment 115, 2861–2873.

Mitchard, E.T.A., Saatchi, S.S., Woodhouse, I.H., Nangendo, G., Ribeiro, N.S., Williams, M., Ryan, C.M., Lewis, S.L., Feldpausch, T.R., Meir, P., 2009. Using satellite radar backscatter to predict above-ground woody biomass: a consistent relationship across four different African landscapes. Geophysical Research Letters 36, L23401.

Mougin, E., Lopes, A., Karam, M.A., Fung, A.K., 1993. Effect of tree structure on X-band microwave signature of conifers. IEEE Transactions on Geoscience and Remote Sensing 31, 655–667.

Niklas, K.J., 1994. Plant Allometry: The Scaling of Form and Process. University of Chicago Press.

Niklas, K.J., Midgley, J.J., Rand, R.H., 2003. Tree size frequency distributions, plant density, age and community disturbance. Ecology Letters 6, 405–411.

Papathanassiou, K.P., Cloude, S.R., 2001. Single-baseline polarimetric SAR interferometry. IEEE Transactions on Geoscience and Remote Sensing 39, 2352–2363.

Patenaude, G., Milne, R., Dawson, T.P., 2005. Synthesis of remote sensing approaches for forest carbon estimation: reporting to the Kyoto Protocol. Environmental Science & Policy 8, 161–178.

Peake, W., 1959. Theory of Radar Return From Terrain. IRE National Convention Record, pp. 27–41.

Philip, M.S., 1994. Measuring Trees and Forests, 2nd ed. CAB International, Wallingford, U.K.

Ranson, K.J., Saatchi, S., Sun, G., 1995. Boreal forest ecosystem characterization with SIR-C/XSAR. IEEE Transactions on Geoscience and Remote Sensing 33, 867–876.

Ranson, K.J., Sun, G., 1994. Mapping biomass of a northern forest using multifrequency SAR data. IEEE Transactions on Geoscience and Remote Sensing 32, 388–396.

Saatchi, S.S., McDonald, K.C., 1997. Coherent effects in microwave backscattering models for forest canopies. IEEE Transactions on Geoscience and Remote Sensing 35, 1032–1044.

Saatchi, S.S., McDonald, K.C., 2002. Coherent effects in microwave backscattering models for forest canopies. IEEE Transactions on Geoscience and Remote Sensing 35, 1032–1044.

Sankaran, M., Ratnam, J., Hanan, N., 2008. Woody cover in African savannas: the role of resources, fire and herbivory. Global Ecology and Biogeography 17, 236–245.

Shula, R.G., 1989. The upper limits of radiata pine stem-volume production in NZ. New Zealand Forestry, 19–22.

Smith-Jonforsen, G., Folkesson, K., Hallberg, B., Ulander, L.M.H., 2007. Effects of forest biomass and stand consolidation on P-band backscatter. IEEE Geoscience and Remote Sensing Letters 4, 669.

Smith, G., 2000. Radar Remote Sensing of Forests Using CARABAS and ERS. Chalmers University of Technology, Gothenburg.

Smith, G., Ulander, L.M.H., 1998. Forest biomass retrieval using VHF SAR, vol. 441. European Space Agency-Publications – ESA SP, pp. 301–308.

Smith, G., Ulander, L.M.H., 2000. A model relating VHF-band backscatter to stem volume of coniferous boreal forest. IEEE Transactions on Geoscience and Remote Sensing 38, 728–740.

Smith, G., Ulander, L.M.H., Fransson, J.E.S., Walter, F., Gustavsson, A., 2002. Forest stem volume retrieval with VHF-band SAR. In: Proceedings of the Third International Symposium on Retrieval of Bio- and Geophysical Parameters from SAR Data for Land Applications, pp. 13–18.

Tang, K., Dimenna, R.A., Buckius, R.O., 1996. Regions of validity of the geometric optics approximation for angular scattering from very rough surfaces. International Journal of Heat and Mass Transfer 40, 49–59.

Treuhaft, R.N., Madsen, S.N., Moghaddam, M., van Zyl, J.J., 1996. Vegetation characteristics and underlying topography from interferometric radar. Radio Science 31.

Valentine, H.T., Tritton, L.M., Furnival, G.M., 1984. Subsampling trees for biomass, volume, or mineral content. Forest Science 30, 673–681.

Waring, R.H., 1983. Estimating Forest Growth and Efficiency in Relation to Canopy Leaf Area. Academic Press.

West, G.B., Brown, J.H., Enquist, B.J., 1997. A general model for the origin of allometric scaling laws in biology. Science 276, 122.

West, G.B., Brown, J.H., Enquist, B.J., 1999. The fourth dimension of life: fractal geometry and allometric scaling of organisms. Science 284, 1677.

Woodhouse, I.H., 2006. Predicting backscatter–biomass and height–biomass trends using a macroecology model. IEEE Transactions on Geoscience and Remote Sensing 44, 871–877.

Woodhouse, I.H., Hoekman, D.H., 2000. Radar modelling of coniferous forest using a tree growth model. International Journal of Remote Sensing 21, 1725–1737.

Zianis, D., Mencuccini, M., 2004. On simplifying allometric analyses of forest biomass. Forest Ecology and Management 187, 311–332.